Journal of Advanced Research in Applied Sciences and Engineering Technology

Journal homepage:
https://semarakilmu.com.my/journals/index.php/applied_sciences_eng_tech/index
ISSN: 2462-1943

# A Brief Comparison of Self-Weight Deflection and Optical Path Difference of Lens Mount for Space Applications

Fatouma Maamar[1,*], Abdeldjelil Mankour[1], Omar Mertad[1]

[1] Space Mechanical Research Department, Satellites Development Centre, Algeria Space Agency, BP 4065, Ibn Rochd, USTO, Oran, POS 50 ILOT T12 Bir El Djir, Oran 31130, Algeria

**ABSTRACT**

Optomechanical lenses can experience varying levels of stress, which can have a notable impact on optical parametric systems. To ensure proper alignment, positioning, and location of lens components within design tolerances, it is crucial to have a robust support structure in place for optical systems. The primary load on lens assemblies typically comes from their own weight in different gravity orientations. This study employs an analytical approach to examine the effects of stress resulting from lens mounting on the wave front passing through the lens, which can alter the optical path. Additionally, when an elastomer-mounted lens bears weight, the elastomer can bend, causing the lens to move and the optical axis to become de-centred. Through the use of these analytical methods, designers can identify potential issues with optical elements and mounting conditions, allowing them to take steps to minimize stress. The study's findings underscore the substantial differences in optical path and self-weight deflection between analytical and ideal methods.

***Keywords:***
Opto-mechanical; bonded optic; stress optic coefficient; SAG; OPD; self-weight distortion

## 1. Introduction

The increasing use of opto-mechanical systems in modern technology has motivated the analytical method presented in this paper. These systems often comprise multiple components, including elastomers, glasses, and metals, which are intentionally combined to achieve unique performance characteristics not possessed by any individual component. These systems are exposed to various environmental conditions that can result in issues such as stress, deformation, and bond failure, which frequently play a significant or even primary role. Although existing computer programs that utilize direct numerical methods can provide solutions to such problems, there are benefits to using analytical manipulation. The asymptotic solutions presented in this paper allow for the analysis and grouping of multiple physical variables into a few significant parameters, which can be useful for analytical studies of lens mounts.

* *Corresponding author.*
*E-mail address: fmaamar@cds.asal.dz*

https://doi.org/10.37934/araset.55.2.4354

Several articles discuss lens mounts for use in space applications, and earlier studies on optical path difference and self-weight deflection in lens mounts are summarized in several books [1-8]. The primary focus of lens assembly design, as of 1994, has been on three key areas: maintaining lens position and alignment within the barrel, minimizing stress to prevent lens fracture, and minimizing mechanical deformations that cause distortion in the optical wave front [9-11]. Lens decentring and spacing errors, as well as mechanical deformations, are significant contributors to performance degradation in optical systems. These references provide a comprehensive overview of the current state of lens assembly design.

This study proposes an analytical approach to determine stress birefringence, a phenomenon that changes the index of refraction of an optically isotropic material due to applied stress. Stress birefringence causes general image degradation and alters the polarization of the incident wave front, making the lens act as a varying retarder. To achieve accurate results, various computational methods were employed and compared based on lens deflection and optical path difference for different lens approaches. The ideal design requires minimal assembly tolerances and optimized location, position, and alignment of each lens to withstand adverse environments. However, achieving such conditions can be challenging, especially with increasing performance demands.

## 2. Lens Assembly Design

The schematic in Figure 1. Depicts a simple and effective technique for mounting lenses in a barrel. This serves as an excellent example for analysing optomechanical assemblies that include both lenses and a barrel. The mounting structure in this technique uses epoxy adhesive bonding to fix each lens securely in place.

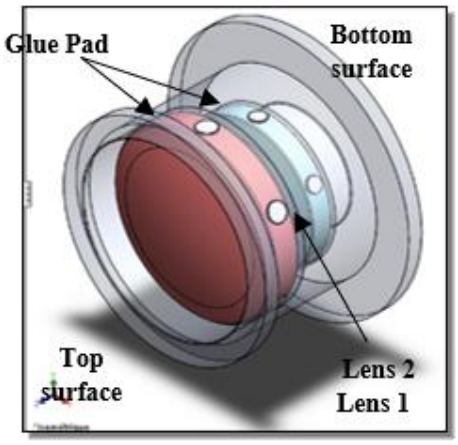


**Fig. 1.** Lens mounting configuration

Lens 1 is a double-convex lens made of N-SF11 glass, which has a high index of refraction and a good stress optical coefficient. Similarly, Lens 2 is bi-convex and made of N-K5 glass, which has a decreased index of refraction but a good stress optical coefficient. Both lenses have two surfaces with positive spherical contours, and in either design, the edge thickness is always less than the centre thickness (refer to Figure 2).

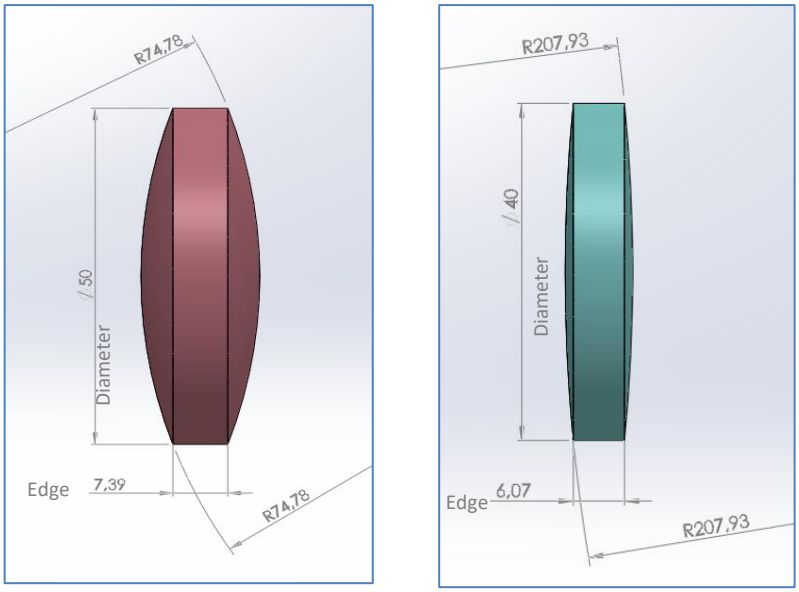


(a) (b)

**Fig. 2.** Description parameters for lenses; a) Lens 1 and b) Lens 2

The rims of the lenses are spherical, ground to minimize the risk of failure upon insertion into a barrel. Table 1 presents the design parameters of the assembly.

**Table 1**
Design parameters for configuration in Figure 1

| Parameter | Lens 1 | Lens2 |
|---|---|---|
| Lens Shape | Double-convex | Double-convex |
| Substrate material | N-SF11 | N-K5 |
| Diameter, D | 50mm | 40mm |
| Radius of curvature, r | 74.78mm | 207.93mm |

Elastic materials, including elastomers, are commonly employed for suspending lens mounts, resulting in athermal assemblies in the radial direction that resist stress build-up caused by differential expansion or contraction. The ideal thickness of the athermal radial elastomer can be determined using the Bayar equation [12-14]:

$$h_{r,Bayar} = r_{optic} \frac{\propto_m - \propto_{optic}}{\propto_G - \propto_m} \quad (1)$$

Where:

- $r_{optic}$ , is the lens ratio in mm
- $\alpha_{optic}$ , is the thermal expansion coefficient of the lens (ppm/°C)
- $\alpha_m$ , is the thermal expansion coefficient of the barrel (ppm/°C)
- $\alpha_G$ , is the thermal expansion coefficient of the glue pad (ppm/°C)

The Bayar equation neglects the impact of Poisson's ratio and elastomer confinement, both of which become more significant as the thickness-to-length ratio of the elastomer bond increases. As such, Eq. (1) is merely an approximation that is suitable for initial analysis. It is also useful for creating discrete bond pads or a series of non-continuous bonds around the lens where the elastomer is not confined.

Deluzio [15,16] presents an equation to athermal size adhesive bonds expressed in Eq. (2).

$$h_{r,Deluzio} = r_{optic} \frac{1-\nu_G}{1+\nu_G} . \left[ \frac{\alpha_m - \alpha_{optic}}{(\alpha_G - \alpha_{optic}) - \frac{(7-6\nu_G).(\alpha_m - \alpha_{optic})}{4.(1+\nu_G)}} \right] \quad (2)$$

When assembling a lens, it is essential to consider the acceleration forces caused by gravity, and the axial position of the lens within the mount must be held constant during such exposure. To achieve this, the axial force exerted by the retainer must be constrained by an axial preload, P, as determined by the following equation [17]:

$$P = 9.81.W.A \quad (3)$$

where:
− P, is in Newtons (N)
− W, is the weight of lens component in Kg
−A, is maximum imposed acceleration factor

To calculate the weight of the lens, begin by determining its volume. This can be achieved by calculating the volume of the primitive shapes, such as the convex shape for surface 1, cylindrical shape for the main part of the lens, and convex shape for surface 2. The volume of the spherical surfaces 1 and 2 can be determined as follows:

$$VOL_1 = \pi . SAG_1^2 \left( r_1 - \frac{SAG_1}{3} \right) \quad (4)$$

$$VOL_2 = \pi . SAG_2^2 \left( r_2 - \frac{SAG_2}{3} \right) \quad (5)$$

where:
− $SAG_1$ , The sagittal thickness of the surface 1 in mm
− $SAG_2$ , The sagittal thickness of the surface 2 in mm
− $r_1$ , Lens radius of curvature, surface 1 in mm
− $r_2$ , Lens radius of curvature, surface 2 in mm

The Sag or Sagitta of a lens is the distance from the centre of its surface to the mounting flat along the optical axis. The thickness of the two surfaces in the sagittal direction can be calculated using the following equation:

$$SAG_1 = r_1^2 - \sqrt{r_1^2 - \left(\frac{D}{2}\right)^2} \quad (6)$$

$$SAG_2 = r_2^2 - \sqrt{r_2^2 - \left(\frac{D}{2}\right)^2} \quad (7)$$

where: D, is lens diameter in mm. The volume of the cylindrical section of the lens is given by:

$$VOL_{CE} = \pi . H . \frac{D^2}{4} \quad (8)$$

where: H, is the edge thickness of the lens in mm

$$H = h - SAG_2 + SAG_1 \quad (9)$$

where: h, is axial thickness of lens in mm. The exact weight of the lens is then:

$$W = \rho.(VOL_{CE} - VOL_1 + VOL_2) \quad (10)$$

where: ρ, is mass density of the lens (Kg/m3). By utilizing the geometry depicted in Figure 1 and data extracted from Table 1 and Table 2, we can calculate the ideal radial thickness of adhesive required for athermalizing the lens (as shown in Table 3).

**Table 2**
Parameters defining the materials [18-21]

| Part | Barrel | Glue Pad | Lens 1 | Lens 2 |
|---|---|---|---|---|
| Material | Aluminium | Epoxy | N-SF11 | N-K5 |
| Young's Modulus E(MPa) | 69000 | 72.44 | 92000 | 71000 |
| Shear Modulus G (MPa) | 28750 | 25.054 | 36595 | 29003 |
| Poisson's Ration υ | 0.2 | 0.39 | 0.257 | 0.224 |
| Coefficient of Thermal Expansion α ($10^{-6}$ (/K)) | 0.23 | 102 | 8.5 | 8.2 |
| Stress-optic Coefficient, Ks (10-6($MPa^{-1}$)) | - | - | 1.33 | 3.03 |
| Mass Density, ρ ($Kg/m^3$) | 2801 | 1260 | 3220 | 2590 |

**Table 3**
The optimum radial thickness of the adhesive to athermalize the lens

| | Optimum Radial thickness of adhesive, hr (mm) | |
|---|---|---|
| | Lens 1 | Lens 2 |
| Equation. Bayar | 2.0315 | 1.5663 |
| Equation. Deluzio | 0.9166 | 0.7063 |

This information is then used to compute the total preload and volume of primitive shapes, enabling us to determine the weight of the lens. According to Table 4, the weight of lens 1 is found to be 0.1011 Kg, while the weight of lens 2 is 0.0260 Kg.

**Table 4**
The preload force on the lens

| | Lens 1 | Lens 2 |
|---|---|---|
| | The Sagittal Thickness of the lens SAG (mm) | |
| Surface 1 | 4.3027 | 0.9640 |
| Surface 2 | 4.3027 | 0.9640 |
| - | The volume of the Spherical of the lens Vol (mm3) | |
| Surface 1 | 4263.72 | 605.922 |
| Surface 2 | 4263.72 | 605.922 |
| The volume of cylindrical of the lens Vol $_{CE}$ ($mm^3$) | 31400 | 10048 |
| The edge thickness of the lens H (mm) | 16 | 8 |
| The weight of the lens W(Kg) | 0.1011 | 0.0260 |
| The preload force on the lens P(N) | 3.9675 | 1.0212 |

## 3. Analytical Solution

### *3.1 Self-Weight Deflection*

Optomechanics is a field within optical engineering that aims to identify environmental conditions that may impact the performance of an optical system, as per specific requirements. Temperature, pressure, vibration, and shock are among the most important conditions that can exert static or dynamic forces on hardware components, potentially leading to deflections or dimensional changes. Such effects can result in misalignment, adverse internal stresses, birefringence, optic breakage, or mechanical deformation. When a lens is vertically mounted, for instance, its own weight may cause deformations, referred to as self-weight deflection, which may compromise performance. A structure exhibiting self-weight deflection that is less than the alignment tolerance is considered stiff, while a structure whose self-weight deflection exceeds the alignment tolerance is compliant. Additionally, under radial acceleration, a lens surrounded by an elastomer can displace radially, with the radial self-weight deflection of the lens (de-centre) are taken from the previous studies [17,22-24]:

$$\delta = \frac{W.9{,}81}{\left[\frac{\pi}{2}.D.\frac{h}{h_r}.\left(\frac{E_{Glue}}{1-\nu_{Glue}^2}+G_{Glue}\right)\right]} \tag{11}$$

This formula enables a swift estimation of a lens' self-weight deflection when mounted vertically, accounting for its weight. The formula's accuracy is dependent on the optimal athermal radial thickness of adhesive. Table 5 provides the self-weight deflection, measured in micrometres, for each lens element using two different radial thicknesses of adhesive as per the Bayar and Deluzio equation.

**Table 5**
Self-weight deflection for each element 'lenses' in meter

| Glasses | | Lens 1 | Lens 2 |
|---|---|---|---|
| Deflection (μm) | hr, Bayar | 1.49 | 0.737 |
| | hr, Deluzio | 0.670 | 0.332 |

In this assembly, the elastic deformation of the elastomer under normal gravity and acceleration causes radial de-centres in the lenses' elements. The Bayar equation is used with radial thicknesses of 2.0315mm and 1.5663mm for lens 1 and 2, respectively, to determine the radial de-centres. By using the Deluzio equation, the optimal athermal bonds are found to be 1.5663mm and 0.7063mm for lens 1 and 2, respectively. It can be concluded that the worst-case self-weight decentration of either of the two lenses in this assembly will not exceed 2μm, which is significantly smaller than the corresponding decentration tolerance of 10μm.

The self-weight deflection falls comfortably below the tolerance even for a high-performance lens. The findings indicate that athermal bonds created using compliant adhesives are highly susceptible to changes in bond thickness. However, radial de-centre does not appear to be a concern.

### *3.2 Optical Path Difference*

The optical path difference (OPD) that occurs when two perpendicularly polarized wave fronts pass through stressed glass arises from the material's stress optic coefficients. The total magnitude of the OPD is what matters, and this is determined by summing the two stress optic coefficients to

obtain a single coefficient, known as Ks. Ks is typically measured in inverse megapascals (1/MPa) and varies from 1.33.10-6 MPa-1 for glass N-SF11 to 3.03.10-6 MPa-1 for glass N-K5. For a given glass thickness (h) and stress level (σ) [6,7,25], the OPD resulting from the stress optic effect can be calculated using the following formula:

$$\mathrm{OPD} = \mathrm{K_s}.\mathrm{h}.\sigma \tag{12}$$

The stress induced at the interface between the lens and mount is highly localized and does not extend far into the clear aperture. As a worst-case analysis, the stresses in the lens are root-sum-squared and applied at the thickest part of the lens to determine the maximum stress optic OPD [6]:

$$\mathrm{OPD_{max}} = \mathrm{k_s}.\mathrm{h}.\left(\sum_{\mathrm{i}=1}^{\mathrm{N}} \sigma_{\mathrm{i}}^2\right)^{1/2} \tag{13}$$

Where OPD max is the maximum stress optic OPD, h is the axial thickness of lens, σi is the individual stress, and N is the number of stresses [17].

$$\sigma_{\mathrm{i}} = (\sigma_{\mathrm{AB}}^2 + \sigma_{\mathrm{c1}}^2 + \sigma_{\mathrm{c2}}^2 + \sigma_{\mathrm{R}}^2)^{1/2} \tag{14}$$

$\sigma_{c1}$: The contact stress in the lens due to a tangential retainer of surface 1.

$$\sigma_{\mathrm{c1}} = 0.798.\left[\frac{\frac{\mathrm{P}}{2.\pi.\mathrm{y}.2.\mathrm{r}_{1,\mathrm{lens}}}}{\left(\frac{1-\nu_{\mathrm{lens}}^2}{\mathrm{E_{lens}}}\right)+\left(\frac{1-\nu_{\mathrm{barrel}}^2}{\mathrm{E_{barrel}}}\right)}\right]^{0.5} \tag{14.1}$$

$\sigma_{c2}$: The contact stress in the lens due to a tangential retainer of surface 2.

$$\sigma_{\mathrm{c2}} = 0.798.\left[\frac{\frac{\mathrm{P}}{2.\pi.\mathrm{y}.2.\mathrm{r}_{2,\mathrm{lens}}}}{\left(\frac{1-\nu_{\mathrm{lens}}^2}{\mathrm{E_{lens}}}\right)+\left(\frac{1-\nu_{\mathrm{barrel}}^2}{\mathrm{E_{barrel}}}\right)}\right]^{0.5} \tag{14.2}$$

$\sigma_R$: The radial wall stress in the lens due to temperature drop.

$$\sigma_R = \frac{K_R.(\alpha_{barrel}-\alpha_{lens}).\Delta T}{\frac{1}{E_{lens}}+\frac{D_{lens}}{2.E_{barrel}.h_m}}$$
$$K_R = 1 - \frac{\Delta r}{\frac{D_{lens}}{2}.\Delta T.(\alpha_{barrel}-\alpha_{lens})} \tag{14.3}$$

$\sigma_{AB}$: Axial stress due to temperature drop, Bayer's method.

$$\sigma_{AB} = \frac{(\alpha_{barral}-\alpha_{lens}).E_{barrel}.E_{lens}.\Delta T}{E_{barrel}+E_{lens}} \tag{14.4}$$

$\sigma_{AY}$: Axial stress due to temperature drop, Yoder's method.

$$\sigma_{AY} = \frac{E_{lens}.E_{barrel}.A_m.(\alpha_{barrel}-\alpha_{lens}).\Delta T}{2.\left(\frac{E_{lens}.A_G}{2}+E_{barrel}.A_m\right)}$$

$$A_G = 2.\pi.y.t_E \quad A_m = 2.\pi.h_m.\left(\frac{D_{lens}+2\Delta r}{2}+\frac{h_m}{2}\right) \tag{14.5}$$

$OPD_B$: OPD using results from Bayar's method.

$$OPD_B = k_s.h.(\sigma_{AB}^2+\sigma_{c1}^2+\sigma_{c2}^2+\sigma_R^2)^{1/2} \tag{15}$$

$OPD_Y$: OPD using results from Yoder's method.

$$OPD_Y = k_s.h.(\sigma_{AY}^2+\sigma_{c1}^2+\sigma_{c2}^2+\sigma_R^2)^{1/2} \tag{16}$$

The unit of optical path difference is meter for the two states of polarized light (perpendicular and parallel) due to a given amount of mechanical stress at a given temperature (Table 6).

**Table 6**
The values of the OPD for each element lenses in meter

| Method used | Optical path difference | |
|---|---|---|
| | Lens 1 | Lens 2 |
| OPD_Bayar's Method | 3.46 $e^{-7}$ | 3.42 $e^{-7}$ |
| OPD_Yoder's Method | 3.52 $e^{-7}$ | 3.38 $e^{-7}$ |
| OPD (m)/ h_Deluzio Equation | 7.18 $e^{-7}$ | 8.06 $e^{-7}$ |

We compute birefringence in the region of the lens and then the total maximum OPD associated with this stress (Table 7).

**Table 7**
The maximum stress optic OPD

| Method used | Permissible OPD/cm Glass path (nm/cm) | |
|---|---|---|
| | Lens 1 | Lens 2 |
| OPD_Bayar's Method | 3.46 | 3.42 |
| OPD_Yoder's Method | 3.52 | 3.38 |
| OPD (m)/ h_Deluzio Equation | 7.18 | 8.06 |

The findings presented in the above table indicate that the maximum optical path difference (OPD) is directly proportional to the stress optic coefficient of the optomechanical system. Additionally, the OPD values for both lenses exhibit a significant reduction and fall well below the normal quarter tolerance [6] for diffraction-limited systems.

Tolerances for birefringence are typically defined in terms of the acceptable optical path difference (OPD) and the polarization states of transmitted light at a specific wavelength. In their work, Kimmel and Parks [26,27] found that components for precision instruments such as photolithography optics and astronomical telescopes have a birefringence tolerance of 5nm/cm. Camera, visual telescope, and microscope objectives have a tolerance of 10nm/cm, while eyepieces and viewfinders have a tolerance of 20nm/cm. For condenser lenses and illumination systems with less stringent requirements, lower quality materials may be used.

Based on the temperature conditions of 20°C and -30°C, the desired birefringence for the lens assembly is less than 10nm/cm to maintain the projected performance. However, this level of optical path difference (OPD) would only be marginally acceptable.

## 4. Comparison and Discussion

We compared two types of mounting designs and identified the design shown here. The thickness of the bonds was calculated using the Bayar and Deluzio equation (Eq. (1) – Eq. (2)). To assess the performance of the lens mounting relative to the conventional design, we compared Figures 3 to 4, specifically views (a) to (d). The optical path difference (OPD) was calculated using different equations (Eq. (12) to Eq. (16)) and plotted in Figure 3. Meanwhile, the surface deflection was obtained from two different equations (Eq. (11)) and plotted in Figure 4.

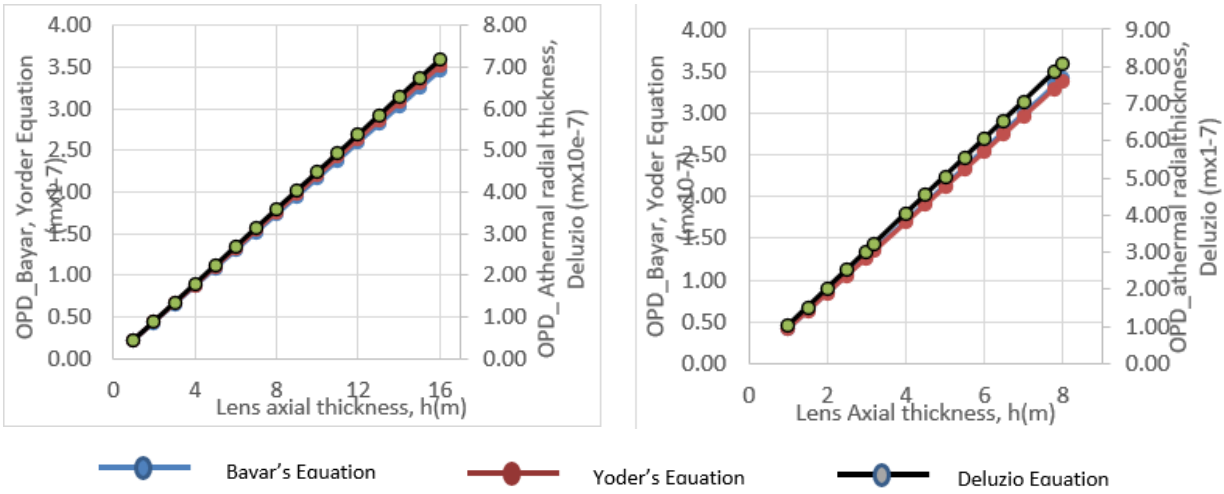


(a) Lens 1 (b) Lens 2

**Fig. 3.** Optical path difference curve as a function the lens axial thickness

Figures 3 and 4 illustrate that surface deformation and optical path difference distribution at the axial thickness of the lens from 1mm to 16 mm for lens 1 and 1mm to 8 mm for lens 2 are more significant in lens 1 than in lens 2. Both lenses exhibit an increase in optical path difference as the axial thickness increases, regardless of the equation used (Bayar, Yoder, or Deluzio). Similarly, the de-centre decreases as the axial thickness of the lens increases, regardless of the radial thickness of the athermal bond used (Bayar or Deluzio). The deflection distribution is more pronounced at higher levels for both lenses and depends on the weight and mechanical properties of the adhesive. Because adhesives have some elasticity, they tend to restore the lens to its original location and orientation when the acceleration force is removed.

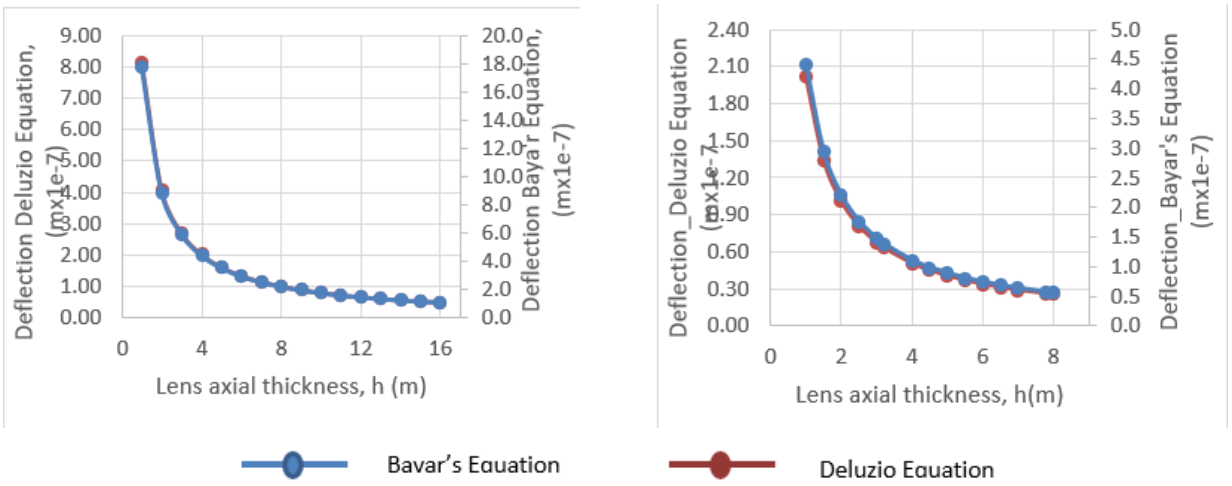


(c) Lens 1 (d) Lens 2

**Fig. 4.** Deflection curve as a function the lens axial thickness

Figures 5 and 6 demonstrate that for lens 1 with an axial thickness of 1mm to 16 mm and lens 2 with an axial thickness of 1 mm to 8 mm, the OPD resulting from self-weight deflection is approximately 0.2 µm and 1.37 µm, respectively. The plots also show that as the optical path difference increases, the surface deflection decreases. Therefore, this mounting lens produces a surface deflection that is mostly free of non-attendance cracks and significantly increases the optical path difference at the lens surface. The study suggests that bonding on a convex glass surface can be considered successful and acceptable.

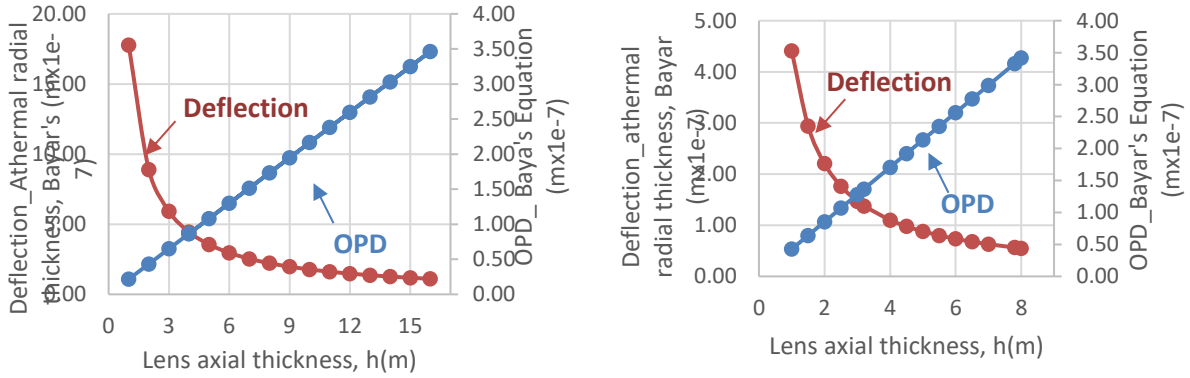


(a) Lens 1 (b) Lens 2

**Fig. 5.** Plots of the surface deflections and resulting OPDs_Bayar Equation and various the lens axial thickness

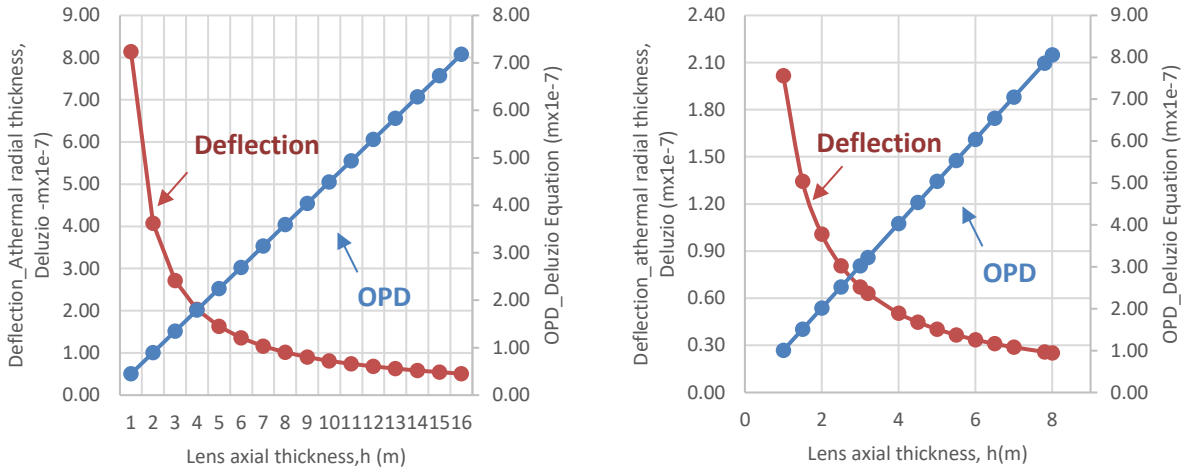


(c) Lens 1 (d) Lens 2

**Fig. 6.** Plots of the surface deflections and resulting OPDs_Deluzio equation and various the lens axial thickness

## 5. Conclusions

The paper's overly optimistic general conclusion should be approached with caution. However, the study demonstrates the importance of minimizing stress levels in the design of lens mounts to minimize the effects of stress birefringence, which is expressed in terms of optical path difference (OPD). The radial elastomeric approach, specifically the Deluzio methodology, is capable of providing an "ideal" lens mount, although performance may be limited.

This research study addresses the analysis of the optical path difference while has led designers to consider the minimization of stress levels to be of prime importance in the design of lens mounts. The conclusion reached by Bayar, Yoder and Deluzio is that stress levels should be minimized in assembly to avoid the effects of stress birefringence which expressed in terms of optical path difference (OPD). Designs that address stress minimization are the radial elastomeric and their deflection produced as a result of the force exerted on the lens, a methodology to calculate the deflection values and OPD for various axial lens thickness configuration is presented. These analytic predictions are generated in graphical form by entering the de-centre and OPD data into an available spreadsheet program. lenses mounted in this article have been shown to exhibit very low deflection and birefringence even regardless approach analytic proposed by Bayar, Yoder and Deluzio.

From an opto-mechanical standpoint, the stresses that could potentially fracture or deform the lens are of primary concern, and closed-form analytical solutions can readily provide these quantities.

## Acknowledgement

This research was funded by a grant from Algerian Space Agency, The Centre of Satellites Development.

## References

[1] Yoder Jr, Paul R. "Advanced considerations of the lens-to-mount interface." In *Optomechanical Design: A Critical Review*, vol. 10265, pp. 276-299. SPIE, 1992. https://doi.org/10.1117/12.61111

[2] Yoder, Paul R. *Mounting optics in optical instruments*. Vol. 181. SPIE press, 2008. https://doi.org/10.1117/3.785236

[3] Yoder Jr, Paul R. *Opto-mechanical systems design*. CRC press, 2005. https://doi.org/10.1201/9781420027235

[4] Vukobratovich, Daniel, Ken A. Fetterhoff, James R. Myers, Paul D. Wheelwright, and George R. Cunnington. "Bonded mounts for small cryogenic optics." In *Infrared Spaceborne Remote Sensing VIII*, vol. 4131, pp. 228-239. SPIE, 2000.

[5] Yoder, Paul R. *Mounting optics in optical instruments*. Vol. 181. SPIE press, 2008. https://doi.org/10.1117/3.785236
[6] Vukobratovich, Daniel, and Paul Yoder. *Fundamentals of optomechanics*. CRC Press, 2018. https://doi.org/10.1201/9781351210867
[7] Vukobratovich, Daniel. "Optomechanical design principles." In *Handbook of Optomechanical Engineering*, pp. 29-52. CRC Press, 2017. https://doi.org/10.1201/9781315216898-2
[8] Ahmad, Anees, ed. *Handbook of optomechanical engineering*. CRC Press, 2017. https://doi.org/10.1201/9781315216898
[9] Paul Jr, R. *Opto-mechanical systems design*. Marcel Dekker, 1993.
[10] Hopkins, Robert E. "Optical element mounting and alignment technique." In *Geometrical Optics*, vol. 531, pp. 187-195. SPIE, 1985. https://doi.org/10.1117/12.946512
[11] Deterding, Leo G. "High-precision, strain-free mounting of large lens elements." *Applied Optics* 1, no. 4 (1962): 403-406. https://doi.org/10.1364/AO.1.000403
[12] Bayar, Mete. "Mechanical design aspects of optomechanical engineering." In *Optical Systems in Engineering I*, vol. 193, pp. 92-100. SPIE, 1979. https://doi.org/10.1117/12.957876
[13] Bayar, Mete. "Lens barrel optomechanical design principles." *Optical Engineering* 20, no. 2 (1981): 181-186. https://doi.org/10.1117/12.7972687
[14] Monti, Christopher L. "Athermal bonded mounts: incorporating aspect ratio into a closed-form solution." In *New Developments in Optomechanics*, vol. 6665, pp. 16-27. SPIE, 2007. https://doi.org/10.1117/12.730275
[15] Deluzio, A.J., "Optimization of elastomer thickness for edge mounted mirrors subject to uniform temperature changes." *Itek*, technical report ATR 68-16 (1968).
[16] Herbert, James J. "Techniques for deriving optimal bondlines for athermal bonded mounts." In *Current Developments in Lens Design and Optical Engineering VII*, vol. 6288, pp. 180-190. SPIE, 2006. https://doi.org/10.1117/12.680828
[17] Vukobratovich, Daniel, and Suzanne M. Vukobratovich. *Introduction to opto-mechanical design*. Raytheon Systems Company, 1999.
[18] Zafri, Mazatul Nadia Mohd, Noraiham Mohamad, Mohd Edeerozey Abd Manaf, Toibah Abd Rahim, Jeefferie Abd Razak, Hairul Effendy Ab Maulod, Qumrul Ahsan, Muhammad Afiq Ani, and Ming Ming Teng. "Vulcanization Bonded Natural Rubber-Aluminum by Chemically Modified Graphene Nanoplatelets-Epoxy Adhesive without Primer." *Journal of Advanced Research in Fluid Mechanics and Thermal Sciences* 110, no. 1 (2023): 182-199. https://doi.org/10.37934/arfmts.110.1.182199
[19] Ma'at, Norzarina, Mohd KhirMohd Nor, Choon Sin Ho, Noradila Abdul Latif, Kamarul-Azhar Kamarudin, Saifulnizan Jamian, Mohd Norihan Ibrahim, and Muhamad Khairudin Awang. "Effects of temperatures and strain rate on the mechanical behaviour of commercial aluminium alloy AA6061." *Journal of Advanced Research in Fluid Mechanics and Thermal Sciences* 54, no. 1 (2019): 21-26.
[20] Ma'at, Norzarina, and Mohd Khir Mohd Nor. "Numerical Analysis of Recycled AA6061 Reinforced Alumina Oxide Undergoing Finite Strain Deformation Uniaxial Tensile and Taylor Cylinder Impact Tests." *Journal of Advanced Research in Fluid Mechanics and Thermal Sciences* 108, no. 2 (2023): 62-76. https://doi.org/10.37934/arfmts.108.2.6276
[21] Rahmani, A., and N. Choupani. "Experimental and numerical analysis of fracture parameters of adhesively bonded joints at low temperatures." *Engineering Fracture Mechanics* 207 (2019): 222-236. https://doi.org/10.1016/j.engfracmech.2018.12.031
[22] Sparks, M., and M. Cottis. "Pressure-induced optical distortion in laser windows." *Journal of Applied Physics* 44, no. 2 (1973): 787-794. https://doi.org/10.1063/1.1662261
[23] Weinswig, Shepard A., and Robert A. Hookman. "Optical analysis of thermal-induced structural distortions." In *Current Developments in Optical Design and Optical Engineering*, vol. 1527, pp. 118-125. SPIE, 1991. https://doi.org/10.1117/12.48643
[24] Roark, Raymond Jefferson. "Formulas for stress and strain." *(No Title)* (1951).
[25] Hsu, Ming-Ying, Shenq-Tsong Chang, and Ting-Ming Huang. "Thermal optical path difference analysis of the telescope correct lens assembly." *Advanced Optical Technologies* 1, no. 6 (2012): 447-453. https://doi.org/10.1515/aot-2012-0058
[26] Kimel, R.K and Parks, R.E., "Preparation of drawings for optical elements and systems: A user's guide." *Optical society of America*, Washington. ISO 10110 optics and optical instruments. (1995).
[27] Doyle, Keith B., Victor L. Genberg, and Gregory J. Michels. "Numerical methods to compute optical errors due to stress birefringence." In *Optical Design and Analysis Software II*, vol. 4769, pp. 34-42. SPIE, 2002. https://doi.org/10.1117/12.481188